

Photophysics of (CdSe)ZnS colloidal quantum dots in an aqueous environment stabilized with amino acids and genetically-modified proteins†

Xin Ai, Qi Xu, Marcus Jones, Qing Song, Shi-you Ding, Randy J. Ellingson, Mike Himmel and Garry Rumbles*

Received 30th April 2007, Accepted 27th June 2007

First published as an Advance Article on the web 10th July 2007

DOI: 10.1039/b706471c

Using a combination of two amino acids, histidine and *N*-acetyl-cysteine, to replace the original organic capping groups of (CdSe)ZnS quantum dots, water-soluble and highly luminescent (CdSe)ZnS quantum dots have been successfully prepared at pH 8. Characterization by steady-state and time-resolved photoluminescence spectroscopy, and transient absorption spectroscopy, demonstrate that the electronic properties of these quantum dots exceed those of the original as-synthesized samples dissolved in a more-conventional organic solvent. Furthermore, these amino acid-stabilized quantum dots have been assembled onto a cellulose substrate *via* cellulose binding proteins that specifically bind to cellulose and was genetically engineered to harbor dual hexahistidine tags at the *N*- and *C*-termini to confer binding with the zinc(II) on the quantum dot surface. The spectroscopic measurements show that the protein-bound quantum dots continue to retain their desirable electronic properties when bound on the substrate. Meanwhile, the specific and very selective binding properties of the proteins have remained effective.

Introduction

The organic ligand bound to the surface of colloidal quantum dots (QDs) plays a pivotal role in determining their electronic and optical properties. A mixture of trioctylphosphine and trioctylphosphine oxide (TOP/TOPO) is the prototypical ligand system for most II-VI and III-V semiconductor systems, such as CdSe and InP.^{1,2} Commonly referred to as the capping group, these ligands provide colloidal stability in common organic solvents such as hexane and toluene. However, these ligands not only provide the all-important solubility, but they serve as agents for reducing the unwanted electronic effects associated with the dangling bonds or surface states, of which the surface of QDs has many. Although there are many examples of the success of this passivation effect, as determined by high photoluminescence (PL) efficiency from the emissive exciton and the absence of emission from the deep trap surface states, there is still good exciton-phonon coupling between the exciton, confined to the QD core, and the long alkyl chains associated with the ligand.³⁻⁶

Providing the QD core with a semiconductor shell that has a wider electronic band gap further decouples the surface states and ligands from the core-bound exciton and although successful in this capacity, it is not a panacea, as the environment still has an impact on the photophysics and spectroscopy of the exciton. There are a number of examples where changing the capping group on, for example, the prototypical (CdSe)ZnS (core)shell QD has a significant impact on the PL quantum efficiency. Replacing TOP/TOPO with mercaptopropionic acid (MPA) is an established procedure⁷ for conferring water solubility (at high pH) on (CdSe)ZnS QDs, but at the expense of a dramatic drop in

PL intensity. This observation has been attributed to coupling of the exciton with the sulfur anion of the deprotonated thiol group that binds to the QD surface.

Water solubility is increasingly recognized as a desirable characteristic as QDs are becoming the system of choice for PL biolabelling applications,⁸⁻¹⁰ and in many cases their greater stability is seeing a usurping of their molecular counterparts, especially in single-species spectroscopies. Whereas they are attractive alternatives to molecular lumiphores, the larger physical size of QDs is not ideal, and the propensity to blink adds an additional problem, although a similar effect is also observed in molecules.¹¹ Highly-luminescent, biocompatible (CdSe)ZnS QDs are now available commercially and often comprise extensive capping structures to enhance the PL efficiency and reduce, but not eliminate, blinking. The surface also has the molecule biotin attached as biotin has a very strong binding coefficient with the protein, avidin, making this a good method of attaching QDs to various entities. Such systems are ideal for labeling studies, but for many applications where physical size is an issue, where a different binding mechanism is to be studied, or where close coupling between the quantum dots is required, this approach is not always appropriate.

Direct binding of proteins to the surface of the QD is an attractive approach to reducing the overall size of the QD-protein combination, and there have been a number of successes using this approach. Using the affinity of histidine for Zn²⁺ ions, proteins with multi-histidine tags on both the *N*- and *C*-termini have been bound successfully to the surface of (CdSe)ZnS quantum dots.^{7,12} Such an approach is very attractive especially if the protein retains its functionality, such as binding to a surface,¹³ and the electronic properties of the quantum dot are fully retained, which often means a good PL efficiency. The affinity of other amino acids to the quantum dot surface is important to understand if the position and mechanism of the binding of the protein to the surface

National Renewable Energy Laboratory, 1617 Cole Blvd, Golden, CO 80401-3393. E-mail: garry_rumbles@nrel.gov

† This paper was published as part of the special issue in honour of David Phillips.

Table 1 pK_a values of histidine, cysteine and *N*-acetyl-cysteine¹⁶

pK_a	-COOH	-NH ⁺ /-SH	-NH ₃ ⁺
Histidine (His)	1.77	6.14	9.24
Cysteine (Cys)	1.82	8.24	10.36
<i>N</i> -Acetyl-cysteine (NAC)	3.08	9.62	—

is to be exploited fully. The role that thiol-containing systems play is of specific interest, as ligands bound to QDs through this nucleophile have been shown to inhibit blinking even in core-shell quantum dots with extensive capping ligand structures.¹⁴ This result indicates that the extensive structures can still be permeated by small molecules, the QD surface is not fully passivated, and that the exciton is still accessible through the semiconductor shell.

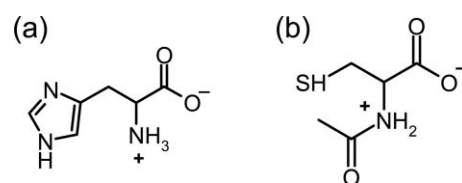
In a recent study,¹⁵ we investigated the photophysics of three amino acids that could bind to the surface of a (CdSe)ZnS quantum dot through a thiol group (cysteine), an amine (lysine) and an imidazole group (histidine). While lysine provided the best PL signal, the pK_a of the conjugate acid of the amine group (pH 10.8) limited solubility to solutions of high pH values only. The advantage of both cysteine and histidine is the pK_a of the nucleophilic group being in the physiologically important pH 6–8 range in which proteins are most stable and still active (Table 1). Whereas QDs solubilized with cysteine gave reasonable PL signals, the solution stability was poor and this was attributed to the oxidation of the $-S^-$ anion to form disulfide bonds. The rate of binding of histidine was found to be very slow, although the small amount of solubilized product exhibited a PL signature similar to that of lysine. This result may explain why a minimum of 5 histidines on the termini of a protein have proven necessary to irreversibly bind the proteins to the zinc-coated QDs.

In this article, we report a detailed study of the photophysics of (CdSe)ZnS quantum dots that have been stabilized with a combination of two amino acids: histidine and *N*-acetyl-cysteine (NAC). We show that this combination readily produces very stable solutions with good PL efficiencies in the pH 6–8 range. We also report the photophysics of the same QDs when bound to a histidine-modified, cellulose-bound protein. We demonstrate that the electronic properties of the QDs are as good, if not better, than the original TOP/TOPO capped species, when solubilized by either the amino acid combination or the protein. We also demonstrate that the protein retains its ability to bind selectively and specifically to a cellulose substrate.

Experimental

Sample preparation

Preparation of E614 QD in amino acid aqueous solution. L-histidine (His, Fluka) and *N*-acetyl-L-cysteine (NAC, Sigma) were used to make an aqueous solution 0.0625 M His–NAC mixture and the pH adjusted to about pH 8.1 using sodium hydroxide. Under these conditions, we expect the structures to be zwitterionic with neutral nucleophiles, as shown in Scheme 1. The (CdSe)ZnS core-shell QDs were purchased from Evident Technologies, and are referred to as E614/TOPO, as the first exciton peak is at 614 nm and it is capped with TOP/TOPO. One hundred μ L of the E614/TOPO in toluene was added to \sim 1.5 mL of methanol to precipitate the QDs out of solution,¹⁷ and the mixture centrifuged

**Scheme 1** Structures of (a) L-histidine (His) and (b) *N*-acetyl-L-cysteine (NAC) at pH 8.

at 13 000 rev min⁻¹ for 15 min. The supernatant was discarded and the QD precipitate re-washed (\times 2) with methanol to wash out all remaining TOP/TOPO molecules. The His–NAC solution was then added to the precipitated QDs and the sample sonicated mildly until most or all of the precipitate reacted and became suspended in the amino acid solution. The suspension was then re-centrifuged to remove any un-reacted solid material and the resulting amino acid-capped QD (called E614/aa) was stored at 4 °C and remained stable for several months.

Cloning and overexpression of recombinant protein. The cellulose binding domain (CBM2) of a cellulase gene derived from *Acidothermus cellulolyticus* was subcloned into expression vectors *via* PCR. The PCR product was cloned into pET28b vector, expressed in *E. coli* BL21 (DE3) at 37 °C, and in the presence of 0.2 mM isopropyl- β -D-thiogalactopyranoside (IPTG). Following growth, the culture was lysed by sonication according to previous procedures.¹⁸ The expressed proteins were identified by SDS-PAGE (10 or 12%) stained by Coomassie brilliant blue. The recombinant proteins were purified by Ni-NTA affinity chromatography (Qiagen) following the manufacturer's specification. Purified CBM2 recombinant protein was kept at 4 °C in the buffer of 50 mM Tris pH of 8.0 with 300 mM NaCl supplemented 20% glycerol.

Preparing bio-conjugates of QD array on cellulose *via* protein. Bacterial microcrystalline cellulose (BMCC) was prepared by a procedure described by Jung *et al.*¹⁹ and was provided by Professor David Wilson (Cornell University). The purified CBM2 (\sim 100 μ g mL⁻¹) was mixed with suspended cellulose (\sim 0.3 mg) in a final volume of 1 mL 50 mM Tris buffer, pH 8.0, with 300 mM NaCl. The mixture was maintained at room temperature for 30 min with gentle rotation, and then centrifuged at 10 000 rev min⁻¹ for 5 min to sediment the cellulose with bound protein. The cellulose particles with bound protein were washed four times with 1 mL aliquots of the His–NAC solution, re-suspended in 1 mL His–NAC solution and then \sim 100 μ L of E614/aa sample was added. The mixture was kept at room temperature for 5 min with gentle rotation, and then centrifuged at 10 000 rev min⁻¹ for 5 min to sediment the cellulose–CBM2–QD complex. This was then washed four times with 1 mL aliquots of the His–NAC solution, and re-suspended in the His–NAC solution after centrifugation. The resulting QD complex is referred as E614/cc2 and was stored at 4 °C for further measurements.

Spectroscopy

Steady-state photoluminescence spectra were recorded using commercial spectrometer (JY Horiba Fluorolog 3) with a 450 W xenon arc lamp and double monochromator as the excitation source. Emission was collected at right angles to excitation through a

spectrograph and detected using a cooled (140 K) CCD multi-channel detector. All spectra were corrected for the intensity of the excitation lamp and wavelength-dependence of the detection system.

Time-resolved photoluminescence measurements were performed using a time-correlated single photon counting spectrometer with a pulsed diode laser (IBH NanoLED-10) operating at 438 nm and at a repetition rate of 1 MHz. Emission was collected at 90° to excitation beam through a 0.22 m monochromator (Spex 1680) fitted with a 1200 lines mm⁻¹ grating and subsequently detected using a photon counting photomultiplier tube (Hamamatsu H6279). The instrument response function (IRF) was measured by detecting scattered excitation light and determined to have a FWHM of 250 ps. Photoluminescence decay counts were accumulated to obtain over 10 000 counts in the channel of maximum intensity and the finite width of the IRF removed using a non-linear least squares iterative re-convolution procedure, with a sum-of-exponentials used as the model fitting function. The quality of fit was judged using a number of stringent statistical criteria including: random distribution of weighted residuals, a goodness-of-fit parameter (reduced chi square) close to 1.0 and a serial correlation coefficient greater than 1.7.

Ultrafast transient absorption (TA) spectra were recorded using a system based on a 1 kHz, 60 fs, 800 nm, amplified Ti:sapphire laser. The fundamental, pulsed output beam was split into two parts, one to generate a pump pulse at 400 nm by second harmonic generation (SHG), the other to pump a 2 mm sapphire window to generate probe pulses of a white-light continuum with wavelengths ranging from 440 nm to 950 nm. Probe pulses were delayed relative to the pump using an optical delay line. The 1S bleaching dynamics were probed at 600 nm. The diameter of the pump beam spot was typically 450 μm at sample, and that of the probe beam less than 150 μm. Typically, the instrument response at the sample was well characterized by a <100 fs FWHM Gaussian function.²⁰ The pump light was set to very low intensity (~6.5 μW) to avoid producing multiple excitons per quantum dot.

Results

TEM images of the E614/TOPO and E614/aa samples are shown in Fig. 1(a) and 1(b), respectively, and the scale bar corresponds to 50 nm. For both images, the concentration of the E614/TOPO sample was adjusted to that of E614/aa as described later. The average size of E614/TOPO QDs is 5 ± 0.2 nm, and the dots are mostly isolated from each other. However, after capped with the His–NAC amino acid combination, the average dot size of E614/aa is still ~5 nm (Fig. 1(b)), but at a similar concentration these dots tend to aggregate and form an ordered, close packed structure.

Introduction of the E614/aa solution to the cellulose fibers with protein assembled on the surface saw the amino acid-capped QDs bind firmly to the protein within minutes. A typical fluorescence microscopy image of the E614/cc2 sample with the fibers luminescing in the red at ~614 nm, the characteristic wavelength associated with the bound E614 QDs. A previous study of these samples has shown that the E614/aa QDs can be assembled on the hydrophobic (1,1,0) face of the cellulose crystals *via* the specific and selective binding ability of the CBM proteins.²¹ The E614/cc2 dots, when bound to the protein on the cellulose, are

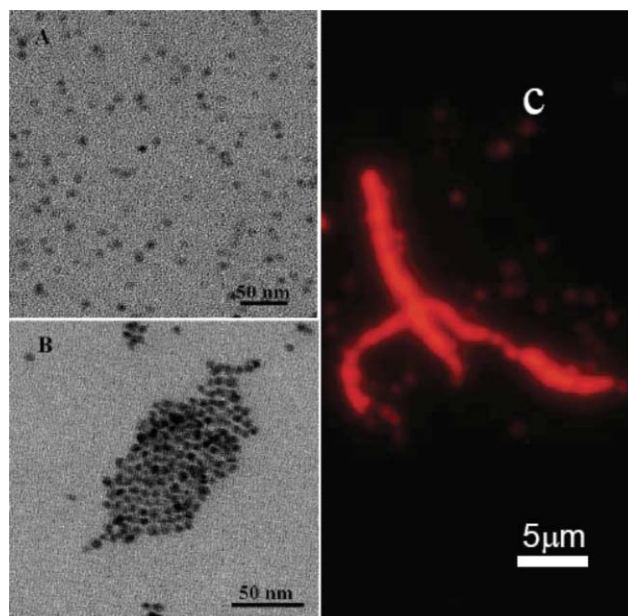


Fig. 1 TEM images of (a) E614/TOPO and (b) E614/aa, and (c) fluorescence microscopy image of E614/cc2.

of the same size as E614/aa and, based on similar studies using a different source of cellulose exhibit an average surface-to-surface, inter-dot distance of 2.6 ± 1.4 nm.²²

Fig. 2 shows the linear absorption spectra of the E614/TOPO and E614/aa solutions. In general, the E614/aa sample shows roughly the same spectrum as that of E614/TOPO with the first exciton absorption peak around 2.07 eV. The typical absorbance at the first exciton peak of E614/aa sample is ~0.04 measured in a 3 mm cuvette, at a concentration that represents the saturated concentration of the suspended (CdSe)ZnS QDs in the amino acid solution. For consistency, the E614/TOPO solution was diluted to have the same optical density as E614/aa at the first exciton peak prior to further spectroscopic characterization. Unfortunately, due to an even lower concentration of QDs and a high scattering background from cellulose fibers, the absorption spectrum of the E614/cc2 sample could not be accurately measured.

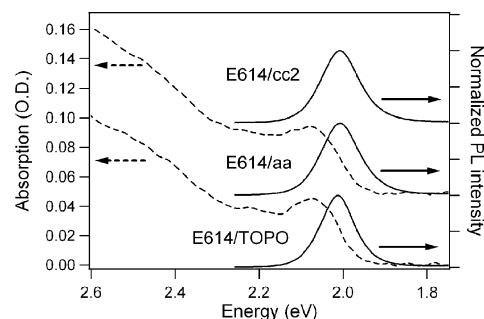


Fig. 2 Normalized absorption and emission spectra of E614/TOPO, E614/aa and E614/cc2.

The normalized steady-state photoluminescence (PL) spectra of the three samples are also shown in Fig. 2, and are re-plotted in Fig. 3 for ease of comparison. As seen in Fig. 3, the E614/aa and E614/cc2 samples exhibit near-identical PL spectra with a maximum at 2.009 eV. Comparing these spectra to that of the

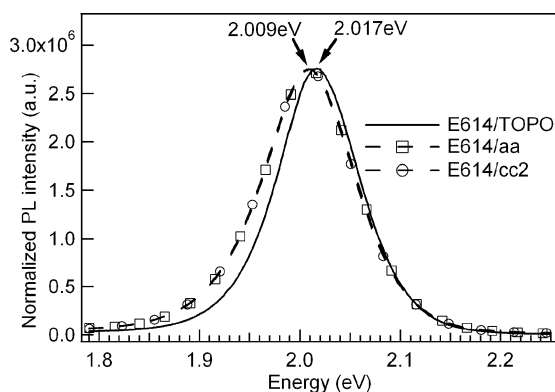


Fig. 3 Normalized, steady-state photoluminescence spectra of E614/TOPO, E614/aa and E614/cc2.

E614/TOPO sample, with a maximum at 2.017 eV, they can be seen to extend further to the red and become broader, with an increase in FWHM of ~ 12 meV. The PL emission yields of E614/TOPO and E614/aa were measured to be 15.5% and 23.4% relative to a perylene fluorescence dye standard (BASF lumogen red in toluene, quantum yield = 1). The quantum yield of E614/cc2 could not be determined accurately due to the inability to record the absorption spectrum, as mentioned earlier.

Fig. 4 compares the normalized time-resolved PL decays of the E614/TOPO, E614/aa and E614/cc2 measured at the exciton emission peak exciting at 438 nm. The decay profiles of both E614/aa and E614/cc2 are longer than for E614/TOPO, whereas E614/cc2 is slightly longer than E614/aa at early time. These data were modeled with 3 exponential decay components according to eqn (1),

$$I(t) = \sum_{n=1}^3 A_n \exp(-t/\tau_n) \quad (1)$$

where τ_n represents a decay time, and A_n the amplitude of this component. The fits are also plotted in Fig. 4 as solid lines. The yield of each decay component was calculated using eqn (2) and along with the other the fitting parameters are tabulated in Table 2.

$$\text{Yield}_n = \frac{A_n \tau_n}{\sum_j A_j \tau_j} \quad (2)$$

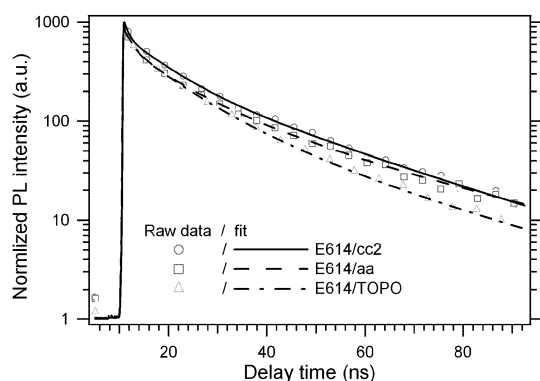


Fig. 4 Normalized, photoluminescence decays (symbols) recorded with excitation at 438 nm and emission detected at the first exciton peak of E614/TOPO, E614/aa and E614/cc2. The solid lines are fits to the data using eqn (1), with the derived coefficients given in Table 2.

Table 2 Three-exponential fitting parameters of PL decays shown in Fig. 3

n	E614/TOPO		E614/aa		E614/cc2	
	τ_n /ps	Yield (%)	τ_n /ps	Yield (%)	τ_n /ps	Yield (%)
1	1706	6.3	1836	6.4	839	3.2
2	10142	50.2	10469	53.9	8040	31.5
3	27187	43.5	32472	53.9	26333	65.3

Transient absorption spectroscopy, a powerful tool to detect carrier dynamics of nanocrystals,^{20,23–25} is also used to measure the three E614 quantum dot samples. Fig. 5 show the transient absorption spectrum (open circles) of E614/aa collected 10 ps after excitation at 400 nm, and the data have been smoothed and the solid line serves as a guide to the eye. The transient spectrum has well resolved bleaching peaks/shoulders at 2.046, 2.183 and 2.460 eV. The bleaching decay dynamics of E614/TOPO, E614/aa and E614/cc2 detected at 2.067 eV with 400 nm excitation were normalized and are shown in Fig. 6. All three samples have identical dynamics at early delay time, with a ~ 400 fs rise time, as shown by the insert. E614/TOPO and E614/aa traces are almost the same for the first 1 ns after excitation, and exhibit non-exponential decay dynamics that can be fit by two decay time components of ~ 100 ps and ~ 3.7 ns. The trace for E614/cc2 shows

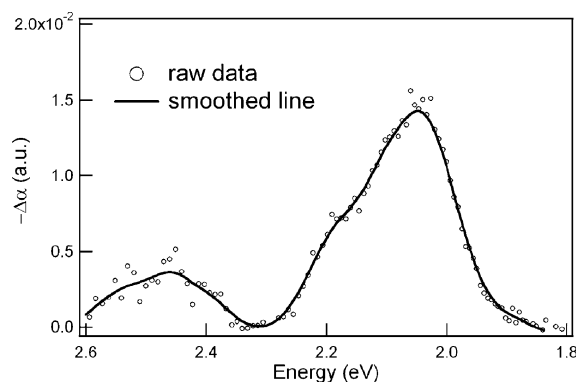


Fig. 5 Transient absorption (bleach) spectrum of E614/aa (open circles, and solid line is the smoothed data) at 10 ps after pumping at 400 nm.

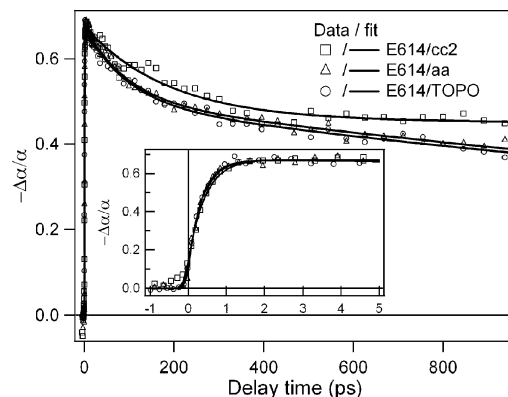


Fig. 6 Normalized TA data (symbols) and fits (solid lines) by multi-exponential function of E614/TOPO, E614/aa and E614/cc2 probed at 2.067 eV with 400 nm pump. The inset shows data in the first 5 ps time window.

Table 3 Two-exponential decay time parameters from the fit to the TA bleaching decay dynamics shown in Fig. 6

<i>n</i>	E614/TOPO		E614/aa		E614/cc2	
	τ_n /ps	A_n (%)	τ_n /ps	A_n (%)	τ_n /ps	A_n (%)
1	97	26.7	94	25.8	188	32.8
2	3636	73.3	3703	74.2	>10 ⁵	67.2

a slightly longer decay that can be fit by a longer time constant, as listed in Table 3.

Discussion

The red shift and broadening of the PL spectrum of E614/aa relative to that of E614/TOPO is quite distinct, even though the absorption spectra of these two samples do not show any distinguishable difference, although this could be a result of the low signal-to-noise ratio at these low concentrations. It is unlikely, however, that the red shift is a result of an increase in size of the (CdSe)ZnS particles, as the capping group exchange takes place at room temperature and there is insufficient energy for the required growth mechanism. From the TEM images in Fig. 1, aggregation of the QDs can be seen in the E614/aa sample, which would explain the red shift,²⁶ while at the same concentration in the E614/TOPO sample image they are quite isolated. However, it is unclear if the E614/aa dots self-assemble on the TEM grid during the evaporation process, or have already aggregated in the amino acid solution. At this pH value (~8), the acid group in solution is deprotonated, but the amine is protonated to give a zwitterionic species, as shown in Scheme 1. In the process of the water evaporation, there could be an attraction between the ionic groups at the end of the ligands resulting in the aggregation phenomenon.

It is possible that the red shift and broadening are associated with solvation effect from different surrounding mediums with different dielectric nature (*e.g.* TOPO–toluene *vs* His–NAC–water). The theoretical study of the factors that influence the excitonic states in QDs has shown that the dielectric confinement effects are as important as quantum confinement effects.²⁷ Experimentally, Leatherdale and Bawendi reported the solvatochromatic shifts in the absorption spectra of CdSe QDs: red shift with increasing dielectric constant of solvent,²⁸ consistent with theoretical prediction. Furthermore, Takagahara also suggested that dielectric confinement effect appears more pronounced for smaller crystallites due to the greater opportunity for the electric force lines to penetrate into the surrounding medium.²⁷ Jin and coworkers²⁹ have observed red-shifted PL spectra of water-soluble (CdSe)ZnS QDs and increasing red shifts with the smaller dots after the TOPO capping group has been exchanged by an amphiphilic calixarene derivative. We also observed a more significant red shift of the PL spectrum (~36 meV) for smaller (CdSe)ZnS QDs (size ≈ 1.9 nm, emission peak at 488 nm) in His–NAC amino acid solution, relative to the original TOP/TOPO capped sample.

The E614/aa sample has a longer average PL decay lifetime than the original E614/TOPO, consistent with the higher PL yield from E614/aa. Since E614/TOPO used for this study is a very dilute solution, it has been suggested³⁰ that the surface bound ligands of dissolved CdSe nanocrystals can dissociate, and the

resulting surface vacancies filled with solvent molecules, leading to a decrease in photoluminescence. In our case, the nanocrystals are a (CdSe)ZnS (core)shell structure, where the shell effectively passivates the surface traps of the CdSe core, and the dilution effect may not therefore be as significant as without a shell. However, the longer average PL lifetime and higher PL yield from the E614/aa sample indicate a better passivation of the surface by the amino acid capping groups; and the capping exchange process preserves and even improves the optical properties of the original source QDs. The E614/cc2 sample has a similar steady-state PL spectrum to E614/aa and an even longer PL decay profile at the early time, concurrent with the longer decay dynamics of the lowest excited state measured by transient absorption spectroscopy as discussed below. This may be attributed to the effective protection of the quantum dot by histidine residues from the protein.

The nonlinear optical response in quantum dots is dominated by state-filling which induces pronounced inter-band bleaching at energies of allowed optical transitions and the transient absorption bleaching features can be assigned by comparison with the linear absorption spectrum.^{24,25} In the transient absorption spectrum of E614/aa collected at 10 ps (Fig. 5), accordingly, the bleaching band around 2.05 eV is assigned to the 1S [1S(e)–1S_{3/2}(h)] transition. The pump light was set to very low intensity to avoid producing multiple excitons per quantum dot, and the magnitude of the state-filling-induced bleaching is therefore proportional to the sum of the electron and hole populations of the quantized states involved in the transition. However, due to the larger effective mass of the hole relative to that of electron ($m_h/m_e = 6$) and the high degeneracy of the valence band, the occupation probability of the lowest electron state at room-temperature is much greater than that of the coupled hole state.²⁵ Therefore, inter band TA signals are dominated by the electron population, and the 1S bleaching dynamics of the E614 QDs collected at 2.067 eV will be used to evaluate the population and depopulation rate of the lowest electron quantized state in those samples.

The rise times of the 1S bleaching dynamics shown in Fig. 6 are associated with the increasing of 1S population, and ascribed to the cooling times of the hot electrons from the higher excited states to the lowest exciton states.^{24,25} It is interesting to note that the three tested samples show a capping-independent cooling time of ~400 fs, that corresponds to an intrinsic carrier cooling time for the CdSe core within the ZnS shell. The decay of the 1S bleaching dynamics describes the depopulation rate of the 1S(e) electron state. The decays associated with E614/aa and E614/TOPO demonstrate similar dynamics represented by two decay components of ~100 ps and 3.7 ns. The faster (100 ps) decay component may be attributed to electron surface trapping, while the nanosecond component is related to the radiative/non-radiative recombination.²⁴ Again, the similar decay dynamics of E614/aa and E614/TOPO are likely a result of the good passivation of the QD surface, as overcoating with a layer of ZnS significantly reduces the number of defects on the QD surface and exchanging the outside capping group should not dramatically affect the relaxation dynamics. Furthermore, the E614/cc sample shows similar but slightly slower decay dynamics, indicating that the good electronic properties of the E614/aa QDs are retained after conjugation to the protein on the cellulose surface. In all three cases, however, the role of the capping group cannot be ignored and the similarity between the data suggests that the amino acid

and amino acid–protein combination are excellent passivators of the surface states.

The binding of the histidine to the surface of the (CdSe)ZnS core-shell nanostructure is ascribed to the histidine–Zn(II) coordination, which is well developed and has been widely used for the purification of tagged recombinant proteins and more recently applied to QD bioconjugation.^{31,32} The pK_a value of the imidazole functional group of histidine is ~ 6.1 ; therefore, at pH 8 it is deprotonated and an imidazole nitrogen can act as a nucleophile and donate its lone pair to the empty orbital of Zn(II) to form a dative bond. Furthermore, it is quite likely that the same mechanism binds the engineered protein, CBM2 with 6X-histidine peptide tags, to the surface of the (CdSe)ZnS quantum dots, with the multi-dentate effect creating a large binding coefficient. It has been shown that ligands with amines can increase the quantum yield of CdSe QDs 2–10 times due to strong electron donating ability of amine nitrogen atom.³³ The use of amine-capped ligands often show an increase in PL intensity for CdSe QDs,^{4,5,15,30} and the same effect may also explain why the E614/aa dots show a higher PL yield and longer PL lifetime.

NAC is a more stable form of L-cysteine probably because it has an acetyl group (CH_3CO) attached that diminishes the cysteine oxidation that impairs the luminescence.^{15,34} It has been proposed that adjacent *N*-acetyl and carboxylate groups stabilize the high electron density, the concomitant high basicity, and the strong reducing power of the thiolate site in NAC.³⁵ The inherent higher electron density of sulfur will facilitate binding with Zn(II), and supply better surface passivation of quantum dots. Previous studies have demonstrated that ligands with thiols act as effective quencher of the band-edge luminescence of CdSe and dramatically diminish the PL yield.^{30,33} However, it has also been proposed that thiolate, not thiol, plays the key role in affecting PL: enhancing PL at low concentration where the thiolate deactivates existing electron trap states, while decreasing PL at high concentration when thiolate acts as a hole trap.³⁶ Gockel and coworkers reported that the acetyl group helps to push pK_a values higher compared to cysteine, for example, pK_R (SH) increases from 8.24 (cys) to 9.62 (NAC).¹⁶ Therefore, at nearly neutral (pH 6–8) environment, less thiolate is expected to be available from NAC than from the cysteine solution, which favors an effective increase in luminescence.

It is interesting to notice that the histidine and NAC mixture produces stable and highly luminescent QD suspensions, whereas the effect of either amino acid alone is not effective. As a borderline between hard and soft Lewis acids,³⁷ Zn^{2+} can bind to both soft thiolate ligands from cysteine (NAC) and harder imidazole ligands from histidine. In nature, cysteine and histidine are actually the predominant ligating units for zinc–amino acid and peptide complexes that take part in all kinds of life processes. For example, Cys2His2 zinc-finger proteins are one of the best known zinc-containing classes of proteins that are involved in nucleic acid binding and gene regulation,³⁸ in which Zn(II) is tetrahedrally coordinated to two cysteine and two histidine residues.

We recently reported²² that a successful array of QDs on cellulose template can be fulfilled *via* engineered CBM proteins, which specifically bind to the hydrophobic planar face of cellulose crystal, possibly through interaction with aromatic amino acid side chains of CBM.³⁹ The two 6XHis-tags fused onto CBM2 protein bind to the Zn(II) on (CdSe)ZnS quantum dot surface likely

via the same binding mechanism as the free histidine discussed above. Therefore, more electron-donating histidine molecules from the His-tags are expected on E614/cc surface and this may also account for the longer, excited state PL lifetime and presumably (not measured) a higher PL emission yield. The result indicates that during the assembling process of QDs onto the cellulose surface, the good surface passivation and electronic properties of E614/aa QDs are preserved and are even improved a little. Meanwhile, the specific binding properties of the proteins onto cellulose have remained effective.

Conclusions

Using a combination of two amino acids, histidine and *N*-acetyl-cysteine, we have successfully exchanged the TOP/TOPO capping groups of (CdSe)ZnS quantum dots, conferring solubility in an aqueous environment at pH 8, which falls in the important physiological pH 6–8 range. Using steady-state and time-resolved PL spectroscopy, and transient absorption spectroscopy, we have demonstrated the electronic properties of these quantum dots are as good, if not better, than the original as-synthesized samples dissolved in a more-conventional organic solvent.

Introducing these quantum dots to a genetically-modified cellulose binding protein (CBM2) bound to a cellulose substrate, the QDs exhibit near-identical photophysical behavior as the unbound QDs. These data demonstrate that the protein-bound QDs also retain the good electronic properties when bound to the substrate, but when combined with the PL imaging data demonstrate that the specific binding properties of the protein have remained effective.

The high dielectric constant of the surrounding aqueous medium induces a solvato-chromic effect that manifests itself as a small red shift and broadening of the emission spectrum, combined with a slight broadening. Otherwise, the electronic properties of the exciton confined to the core of the CdSe quantum dots, remain mostly unaffected; a result that demonstrates both the good confining effect of the ZnS shell combined with the excellent passivating effects of a combination of both the imidazole and thiol nucleophiles.

Acknowledgements

This work was funded by the Photochemistry and Radiation Research program of the U.S. Department of Energy, Office of Science, Basic Energy Sciences, Division of Chemical Sciences, Geosciences and Biosciences, under Contract No. DE-AC36-99GO10337 to NREL.

References

- 1 C. B. Murray, D. J. Norris and M. G. Bawendi, Synthesis And Characterization Of Nearly Monodisperse Cde ($E = \text{S}, \text{Se}, \text{Te}$) Semiconductor Nanocrystallites, *J. Am. Chem. Soc.*, 1993, **115**, 8706–8715.
- 2 O. I. Micic, C. J. Curtis, K. M. Jones, J. R. Sprague and A. J. Nozik, Synthesis And Characterization Of Inp Quantum Dots, *J. Phys. Chem.*, 1994, **98**, 4966–4969.
- 3 M. R. Salvador, M. A. Hines and G. D. Scholes, Exciton-bath coupling and inhomogeneous broadening in the optical spectroscopy of semiconductor quantum dots, *J. Chem. Phys.*, 2003, **118**, 9380–9388.

- 4 C. Landes and M. A. El-Sayed, Thermodynamic and kinetic characterization of the interaction between *N*-butylamine and similar to 1 nm CdSe nanoparticles, *J. Phys. Chem. A*, 2002, **106**, 7621–7627.
- 5 C. Landes, C. Burda, M. Braun and M. A. El-Sayed, Photoluminescence of CdSe nanoparticles in the presence of a hole acceptor: *n*-butylamine, *J. Phys. Chem. B*, 2001, **105**, 2981–2986.
- 6 P. Guyot-Sionnest, B. Wehrenberg and D. Yu, Intraband relaxation in CdSe nanocrystals and the strong influence of the surface ligands, *J. Chem. Phys.*, 2005, **123**, 074709.
- 7 H. Mattoussi, J. M. Mauro, E. R. Goldman, G. P. Anderson, V. C. Sundar, F. V. Mikulec and M. G. Bawendi, Self-assembly of CdSe-ZnS quantum dot bioconjugates using an engineered recombinant protein, *J. Am. Chem. Soc.*, 2000, **122**, 12142–12150.
- 8 W. C. W. Chan, D. J. Maxwell, X. H. Gao, R. E. Bailey, M. Y. Han and S. M. Nie, Luminescent quantum dots for multiplexed biological detection and imaging, *Curr. Opin. Biotechnol.*, 2002, **13**, 40–46.
- 9 B. Dubertret, P. Skourides, D. J. Norris, V. Noireaux, A. H. Brivanlou and A. Libchaber, vivo imaging of quantum dots encapsulated in phospholipid micelles, *Science*, 2002, **298**, 1759–1762.
- 10 M. Bruchez, M. Moronne, P. Gin, S. Weiss and A. P. Alivisatos, Semiconductor nanocrystals as fluorescent biological labels, *Science*, 1998, **281**, 2013–2016.
- 11 C. R. Bagshaw and D. Cherny, Blinking fluorophores: what do they tell us about protein dynamics?, *Biochem. Soc. Trans.*, 2006, **34**, 979–982.
- 12 S. Y. Ding, M. Jones, M. P. Tucker, J. M. Nedeljkovic, J. Wall, M. N. Simon, G. Rumbles and M. E. Himmel, Quantum dot molecules assembled with genetically engineered proteins, *Nano Lett.*, 2003, **3**, 1581–1585.
- 13 S. Y. Ding, G. Rumbles, M. Jones, M. P. Tucker, J. Nedeljkovic, M. N. Simon, J. S. Wall and M. E. Himmel, Bioconjugation of (CdSe)ZnS quantum dots using a genetically engineered multiple polyhistidine tagged cohesin/dockerin protein polymer, *Macromol. Mater. Eng.*, 2004, **289**, 622–628.
- 14 S. Hohng and T. Ha, Near-complete suppression of quantum dot blinking in ambient conditions, *J. Am. Chem. Soc.*, 2004, **126**, 1324–1325.
- 15 M. Jones, S. Y. Ding, M. P. Tucker, Y. H. Kim, S. B. Zhang, M. E. Himmel and G. Rumbles, Stabilization of (CdSe)ZnS Quantum Dots in Water Using Amino Acid Capping Groups, in *205th Meeting of the Electrochemical Society*, ed. G. L. Rumbles and T. Murakoshi, Electrochemical Society Inc., San Antonio, Texas, 2006, pp. 340–349.
- 16 P. Gockel, H. Vahrenkamp and A. D. Zuberbuhler, Zinc-Complexes Of Cysteine, Histidine, And Derivatives Thereof-Potentiometric Determination Of Their Compositions And Stabilities, *Helv. Chim. Acta*, 1993, **76**, 511–520.
- 17 D. Gerion, F. Pinaud, S. C. Williams, W. J. Parak, D. Zanchet, S. Weiss and A. P. Alivisatos, Synthesis and properties of biocompatible water-soluble silica-coated CdSe/ZnS semiconductor quantum dots, *J. Phys. Chem. B*, 2001, **105**, 8861–8871.
- 18 S. Y. Ding, E. A. Bayer, D. Steiner, Y. Shoham and R. Lamed, A novel cellulosomal scaffolding from *Acetivibrio cellulolyticus* that contains a family 9 glycosyl hydrolase, *J. Bacteriol.*, 1999, **181**, 6720–6729.
- 19 H. Jung, D. B. Wilson and L. P. Walker, Binding and reversibility of thermobifida fusca Cel5A, Cel6B, and Cel48A and their respective catalytic domains to bacterial microcrystalline cellulose, *Biotechnol. Bioeng.*, 2003, **84**, 151–159.
- 20 R. J. Ellingson, J. L. Blackburn, J. Nedeljkovic, G. Rumbles, M. Jones, H. X. Fu and A. J. Nozik, Theoretical and experimental investigation of electronic structure and relaxation of colloidal nanocrystalline indium phosphide quantum dots, *Phys. Rev. B*, 2003, **67**, 075308.
- 21 S. Y. Ding, Q. Xu, M. K. Ali, J. O. Baker, E. A. Bayer, Y. Barak, R. Lamed, J. Sugiyama, G. Rumbles and M. E. Himmel, Versatile derivatives of carbohydrate-binding modules for imaging of complex carbohydrates approaching the molecular level of resolution, *Biotechniques*, 2006, **41**, 435.
- 22 Q. Xu, X. Ai, P. Ahrenkiel, M. Jones, M. P. Tucker, G. Rumbles, M. E. Himmel and S. Y. Ding, Bioengineered Carbohydrate-Binding Protein Modules designed to Assemble Linear Arrays of Quantum Dots on Cellulose Nanocrystals, to be submitted.
- 23 P. R. Yu, J. M. Nedeljkovic, P. A. Ahrenkiel, R. J. Ellingson and A. J. Nozik, Size dependent femtosecond electron cooling dynamics in CdSe quantum rods, *Nano Letters*, 2004, **4**, 1089–1092.
- 24 V. I. Klimov, D. W. McBranch, C. A. Leatherdale and M. G. Bawendi, Electron and hole relaxation pathways in semiconductor quantum dots, *Phys. Rev. B*, 1999, **60**, 13740–13749.
- 25 V. I. Klimov, Optical nonlinearities and ultrafast carrier dynamics in semiconductor nanocrystals, *J. Phys. Chem. B*, 2000, **104**, 6112–6123.
- 26 C. B. Murray, C. R. Kagan and M. G. Bawendi, Synthesis and characterization of monodisperse nanocrystals and close-packed nanocrystal assemblies, *Ann. Rev. Mater. Sci.*, 2000, **30**, 545–610.
- 27 T. Takagahara, Effects Of Dielectric Confinement And Electron-Hole Exchange Interaction On Excitonic States In Semiconductor Quantum Dots, *Phys. Rev. B*, 1993, **47**, 4569–4585.
- 28 C. A. Leatherdale and M. G. Bawendi, Observation of solvatochromism in CdSe colloidal quantum dots, *Phys. Rev. B*, 2001, **63**, 165315.
- 29 T. Jin, F. Fujii, E. Yamada, Y. Nodasaka and M. Kinjo, Control of the optical properties of quantum dots by surface coating with calix[n]arene carboxylic acids, *J. Am. Chem. Soc.*, 2006, **128**, 9288–9289.
- 30 G. Kalyuzhny and R. W. Murray, Ligand effects on optical properties of CdSe nanocrystals, *J. Phys. Chem. B*, 2005, **109**, 7012–7021.
- 31 I. L. Medintz, A. R. Clapp, H. Mattoussi, E. R. Goldman, B. Fisher and J. M. Mauro, Self-assembled nanoscale biosensors based on quantum dot FRET donors, *Nat. Mater.*, 2003, **2**, 630–638.
- 32 S. Y. Ding, G. Rumbles, M. Jones, M. P. Tucker, J. Nedeljkovic, M. N. Simon, J. S. Wall and M. E. Himmel, Bioconjugation of (CdSe)ZnS quantum dots using a genetically engineered multiple polyhistidine tagged cohesin/dockerin protein polymer, *Macromol. Mater. Eng.*, 2004, **289**, 622.
- 33 C. Bullen and P. Mulvaney, The effects of chemisorption on the luminescence of CdSe quantum dots, *Langmuir*, 2006, **22**, 3007–3013.
- 34 J. A. Kloepfer, S. E. Bradforth and J. L. Nadeau, Photophysical properties of biologically compatible CdSe quantum dot structures, *J. Phys. Chem. B*, 2005, **109**, 9996–10003.
- 35 B. Noszal, D. Visky and M. Kraszni, Population, acid–base, and redox properties of *N*-acetylcysteine conformers, *J. Med. Chem.*, 2000, **43**, 2176–2182.
- 36 S. Jeong, M. Achermann, J. Nanda, S. Lvanov, V. I. Klimov and J. A. Hollingsworth, Effect of the thiol-thiolate equilibrium on the photophysical properties of aqueous CdSe/ZnS nanocrystal quantum dots, *J. Am. Chem. Soc.*, 2005, **127**, 10126–10127.
- 37 R. G. Pearson, Acids and Bases, *Science*, 1966, **151**, 172–177.
- 38 J. M. Berg and H. A. Godwin, Lessons from zinc-binding peptides, *Ann. Rev. Biophys. Biomol. Struct.*, 1997, **26**, 357–371.
- 39 J. Tormo, R. Lamed, A. J. Chirino, E. Morag, E. A. Bayer, Y. Shoham and T. A. Steitz, Crystal structure of a bacterial family-III cellulose-binding domain: A general mechanism for attachment to cellulose, *EMBO J.*, 1996, **15**, 5739–5751.